Ab-Initio XRPD Crystal Structure and Giant Hysteretic Effect (H_c = 5.9 T) of a New Hybrid Terephthalate-Based Cobalt(II) Magnet†

Zhong-Le Huang,*[,‡,#] Marc Drillon,[‡] Norberto Masciocchi,*[,§,||] Angelo Sironi,[§] Jing-Tai Zhao,[⊥] Pierre Rabu,[‡] and Pierre Panissod[‡]

Institut de Physique et de Chimie des Matériaux de Strasbourg, UMR 75040 du CNRS, 23 rue du Loess, 67037 Strasbourg, France; Dipartimento di Chimica Strutturale e Sterechimica Inorganica e Centro CNR "CSSSCMTBSO", Università di Milano, via Venezian 21, 20133 Milano, Italy; Dipartimento di Scienze Chimiche, Fisiche e Matematiche, Università dell'Insubria, via Lucini 3, 22100 Como, Italy; and Max-Planck-Institut für Chemische Physik Fester Stoffe, Nöthnitzer Strasse 40, 01187 Dresden, Germany

Received May 10, 2000. Revised Manuscript Received June 27, 2000

A new terephthalate-based cobalt hydroxide, $Co_2(OH)_2(C_8H_4O_4)$, was synthesized by the hydrothermal method. Its crystal structure has been determined by ab-initio XRPD methods (monoclinic, $C2/m$, a = 19.943(1), b = 3.2895(1), c = 6.2896(3) Å, β = 95.746(3)°) and fully refined by the Rietveld technique down to R_p = 0.15 for 9301 observed data (178 independent reflections). The terephthalates are coordinated and pillared directly to the cobalt hydroxide layers and thus a three-dimensional framework is formed. Because of the bonds with the terephthalates, two crystallographically inequivalent cobalt sites are found inside the hydroxide layers, with different octahedral orientations. Magnetic studies show that the intralayer exchange interaction between Co(II) ions is ferromagnetic but the whole system orders antiferromagnetically at 48 K with a metamagnetic transition above a threshold field of 0.2 T. The existence of conjugated π electrons in terephthalates explains the antiferromagnetic interactions between the layers. Below 45 K, the compound exhibits a hysteretic metamagnetic loop and a remnant moment that is small down to about 30 K, and then rises suddenly reaching a plateau below 15 K. However, at low temperatures the remnant moment is still only a fraction of the full Co(II) moment, which is a sign of canted antiferromagnetism associated with a non-collinear orientation of the moments between the layers. The magnetization loop shows a giant coercive field of 5.9 T at 4.2 K, which must be related to an extremely large single-ion anisotropy on the Co sites.

I. Introduction

The insertion of carboxylic acids into layered transition metal hydroxides by ways of anion-exchange or coprecipitation has attracted considerable attention in the past few years[1−3] because the organic−inorganic hybrid materials thus formed may be of great interest to both fundamental viewpoint and potential applications in the areas of catalysis,[4] sorption,[5] photochemistry,[6] electrochemistry,[7] or magnetism.[8] Recently, several works have focused on the magnetic properties of a series of hydroxide-based compounds, with formulation $M^{II}(OH)_{2-x}(A^n)_{x/n}\cdot zH_2O$ (M = Co, Cu), exhibiting planar triangular arrays of divalent metal ions.[9] Their structures are usually built from the brucite-like hydroxide $M(OH)_2$ through substituting hydroxyl groups with large organic species (A), located in the space between the layers.[10,11] This ion exchange induces important modification of the interlayer spacing, which depending on the nature and the packing of the organic spacers may be increased up to 40 Å. Various types of

* Corresponding authors.

† Non-SI units are employed: 1 T = 10 000 Oe ≈ 7.96 × 10^5 A m^{-1}; 1 μ_B ≈ 9.3 × 10^{-24} J T^{-1}.

‡ Institut de Physique et de Chimie des Matériaux de Strasbourg.
§ Università di Milano.
|| Università dell'Insubria.
⊥ Max-Planck-Institut für Chemische Physik Fester Stoffe.
Current mailing and e-mail addresses: MPI CPfS, Nöthnitzer Strasse 40, 01187 Dresden, Germany; huang@cpfs.mpg.de. Telephone: 49-351-4646-3320. Fax: 49-351-4646-3002.

(1) Carlino, S. *Solid State Ionics* **1997**, *98*, 73−84.
(2) Newman, S. P.; Jones, W. *New J. Chem.* **1998**, 105−115.
(3) Yamanaka, S.; Sako, T.; Seki, K.; Hattori, M. *Solid State Ionics* **1992**, *53*−*56*, 527−533.
(4) (a) Carrado, K. A.; Forman, J. E.; Botto, R. E.; Winans, R. E. *Chem. Mater.* **1993**, *5*, 472−478. (b) Chibwe, M.; Pinnavaia, T. J. *J. Chem. Soc., Chem. Commun.* **1993**, 278−280.
(5) Dutta, P. K.; Robins, D. S. *Langmuir* **1994**, *10*, 4681−4687.
(6) (a) Ogawa, M.; Kuroda, K. *Chem. Rev.* **1995**, *95*, 399−438. (b) Takaki, K.; Shichi, T.; Usami, H.; Sawaki, Y. *J. Am. Chem. Soc.* **1993**, *115*, 4339−4344.
(7) Shaw, B. R.; Deng, Y. P.; Strillacci, F. E.; Carrado, K. A.; Fessehaie, M. G. *J. Electrochem. Soc.* **1990**, *137*, 3136−3143.
(8) Bujoli-Doeuff, M.; Force, L.; Gadet, V.; Verdaguer, M.; el Malki, K.; de Roy, A.; Besse, J. P.; Renard, J. P. *Mater. Res. Bull.* **1991**, *26*, 577−587.
(9) (a) Laget, V.; Hornick, C.; Rabu, P.; Drillon, M. *J. Mater. Chem.* **1999**, *9*, 169−174. (b) Fujita, W.; Awaga, K.; Yokoyama, T. *Appld. Clay Sci.* **1999**, *15*, 281−303.
(10) (a) Meyn, M.; Beneke, K.; Lagaly, G. *Inorg. Chem.* **1990**, *29*, 5201−5207. (b) Vucelic, M.; Moggridge, G. D.; Jones, W. *J. Phys. Chem.* **1995**, *99*, 8328−8337. (c) Weir, M. R.; Moore, J.; Kydd, R. A. *Chem. Mater.* **1997**, *9*, 1686−1690. (d) Kukkadapu, R. K.; Witkowski, M. S.; Amonette, J. E. *Chem. Mater.* **1997**, *9*, 417.

10.1021/cm000386c CCC: $19.00 © 2000 American Chemical Society
Published on Web 08/19/2000

organic anions (*n*-alkyl carboxylates or sulfates, dicarboxylates, radical anions, and dicyanamides) have been investigated, allowing to stabilize hybrid ferro- or ferrimagnetic networks with ordering temperatures ranging from 10 to 58 K.[11] In particular, the key role of through-space dipolar interactions between magnetic layers has been evidenced for explaining the 3D long-range magnetic order.[12] Recently, difunctional molecules, such as *n*-alkanedioates, were used in order to connect adjacent layers through saturated or unsaturated carbon chains.[13] The results obtained for a series of copper(II) and cobalt(II) compounds highlight the influence of the π electrons on the interlayer coupling.

For the cobalt hydroxide and its derivatives, recent discovery of significant magnetic properties, like high T_c and coercive field,[11d−f] opens new perspectives in the field of organic−inorganic magnets. In the meantime, the layered hybrid materials prepared by the way of ion-exchange reaction or coprecipitation at atmospheric temperature and pressure have usually very bad crystallinity, thus restricting the investigations on the structure−property relationships. Further, for the hybrid cobalt compounds, the existence of multiphases, impurities, and lack of crystal structure have hindered the development and puzzled the interpretation of the magnetic properties. The recently reported compound $Co_4(OH)_2(C_8H_4O_4)_3 \cdot (NH_3)_{1.5} \cdot (H_2O)_{2.5}$ [11f] represents a good example of such a situation. It exhibits very significant magnetic properties, but its poor XRD pattern, and the structural model derived from hazardous analysis of IR spectra, make doubtful the chemical formula and the interpretation of magnetic findings.

With the aim of studying the influence of organic molecules on the intra- and interlayer structural and magnetic properties through their coordination in layered hydroxides,[11−13] we decided to pursue the grafting of terephthalate anion, which, thanks to its planar geometry and constitutional stiffness, may be successfully employed in hydrothermal synthesis through self-assembling of suitable synthons; therefore, in the following, we report on the synthesis, characterization, ab-initio X-ray powder diffraction (XRPD) structure determination and peculiar magnetic properties of the new terephthalate-based pillared cobalt hydroxide, $Co_2(OH)_2(C_8H_4O_4)$. This is the first well-characterized layered hydroxyl derivative containing the terephthalate, hereafter tp, anion.

II. Experimental Section

II.1. Synthesis. $Co_2(OH)_2(C_8H_4O_4)$ was synthesized from $CoCl_2 \cdot 6H_2O$ (Aldrich), terephthalic acid (benzene-1,4-dicarboxylic acid, 98%, Lancaster), and KOH (85%, SDS). 1,3-Diaminopropane (99.9%, Fluka) and piperazine (99.9%, Fluka) were used as structure-directing agents. The starting mixture corresponding to the molar composition 2:3:8:4:120 of $CoCl_2 \cdot 6H_2O$, $CO_2HC_6H_4CO_2H$, KOH, diamine, and H_2O was homogenized and transferred into a 23-mL Teflon-walled Parr acid digestion bomb, and then heated for 64 h at 220 °C under autogenous pressure. The reaction product was collected by filtration, washed with distilled water and anhydrous ethanol, and then dried at 40 °C for 24 h. The final product with nearly 100% yield gives a light pink color and has a size distribution between 0.4 and 1.0 μm.

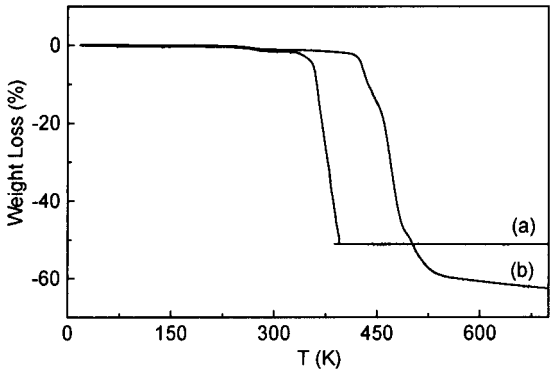

Figure 1. TGA profiles in air (a) and in argon (b) of $Co_2(OH)_2$(tp).

II.2. Physical Measurements. Thermogravimetric and differential thermal (TG-DTA) analyses were performed using a Setaram TGDTA-92 thermobalance. Samples were placed in platinum containers and data were recorded in air and argon between 20 and 700 °C, with a heating rate of 3 °C/min. The data were corrected for the empty container. FTIR spectra were obtained on a ATI Mattson Genesis Series spectrometer in the ranges 400−4000 cm^{-1} (64 scans with a resolution of 4 cm^{-1}, pelleting with KBr). UV−vis spectra were obtained with a Perkin-Elmer UV/vis/NIR spectrometer in the region 200−2500 nm. Samples were prepared as thin film on silica slide. Barium sulfate was used as baseline correction and the data was corrected for the silica slide. X-ray powder diffraction data were collected on a Siemens D500 diffractometer (Co $K\alpha_1$ = 1.788 97 Å) in the 2θ range of 2−102° with an interval of 0.01° and counting time 7 s. The powders were gently ground in an agate mortar and then cautiously deposited in the hollow of a Plexiglas sample holder with the side loading technique[14] which is known to minimize preferred orientation effects in the plane normal to the scattering vector. A Faraday-type pendulum magnetometer with fields up to 1.3 T was used in the range 4−300 K for magnetic susceptibility measurements. A vibrating sample magnetometer (PAR model) was used up to ±1.75 T for isothermal field-dependent magnetization measurements. A Quantum Design SQUID MPMS-XL (maximum field ±5 T in the temperature range 2−300 K) magnetometer was used for both dc and ac magnetic susceptibility and isothermal field-dependent or zero-field temperature-dependent magnetization measurements. High field magnetization up to 20 T was recorded in Grenoble High Magnetic Field Laboratory.

II.3. Characterization. *II.3.1. Elementary Analysis and TG-DTA.* The composition for $Co_2(OH)_2(C_8H_4O_4)$ was checked by chemical analysis (Anal. (Calcd): C, 31.09 (30.39); H, 2.06 (1.90)) and thermogravimetric analysis in air (final product Co_3O_4, Obs. (Calcd): 49.0 (50.8)) and in argon (final product Co, Obs. (Calcd): 37.3 (37.1)).

The TGA trace (Figure 1) shows a decomposition in air into Co_3O_4 at 360 °C, which is exothermic (from DTA curve). In argon, the data indicate an endothermic reaction at about 430 °C, associated with a pyrolysis reduction into Co. The compositions of final products were checked by XRD. Compared with other cobalt compounds, whose thermal decomposition temperature occurs at ∼240 °C,[9,11,13] $Co_2(OH)_2(C_8H_4O_4)$ is thus the most heat resistant in this series of compounds. This behavior

(11) (a) Rabu, P.; Angelov, S.; Legoll, P.; Belaiche, M.; Drillon, M. *Inorg. Chem*. **1993**, *32* (11), 2463−2468. (b) Fujita, W.; Awaga, K. *Inorg. Chem*. **1996**, *35*, 1915−1917. (c) Laget, V.; Rouba, S.; Rabu, P.; Hornick, C.; Drillon, M. *J. Magn. Magn. Mater*. **1996**, *154*, L7−L11. (d) Laget, V.; Hornick, C.; Rabu, P.; Drillon, M.; Ziessel, R. *Coord. Chem. Rev*. **1998**, *178−180*, 1533−1553. (e) Kurmoo, M. *Chem. Mater*. **1999**, *11*, 3370−3378. (f) Kurmoo. M. *Philos. Trans. R. Soc. London A* **1999**, *357*, 3041−3061.

(12) Drillon, M.; Panissod, P. *J. Magn. Magn. Mater*. **1998**, *188*, 93−99.

(13) Hornick, C.; Rabu, P.; Drillon, M. *Polyhedron* **2000**, 259−266.

(14) McMurdie, H. F.; Morris, M.; Evans, E.; Paretzkin, B.; Wong-Ng, W. *Powder Diffr*. **1986**, *1*, 40.

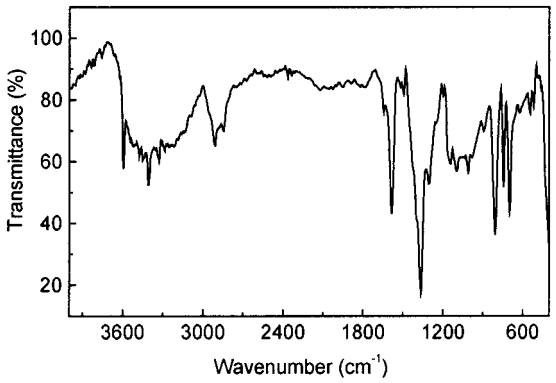

Figure 2. FTIR spectrum (KBr pellets) of $Co_2(OH)_2(tp)$.

Scheme 1

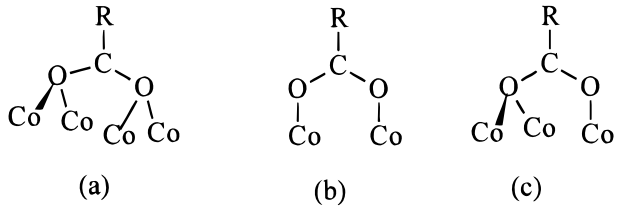

indicates that a strong bond interaction between organic and inorganic components has been achieved by hydrothermal process.

II.3.2. FTIR. FTIR spectra (Figure 2) of $Co_2(OH)_2(C_8H_4O_4)$ clearly shows the stretching vibrations of OH^-, $-COO^-$, and para-aromatic CH group. The assignments of the bands were made according to ref 15. A sharp band at 3594 cm^{-1} is assigned to the stretching vibration of OH groups not involved in hydrogen bonding. Characteristic para-aromatic CH stretching bands are found at 2912, 1142, 1095, 1007, and 810 cm^{-1}. Two intense bands at 1585 and 1365 cm^{-1} are assigned to $\nu_{as}(-COO^-)$ and $\nu_s(-COO^-)$, respectively. The difference between these two bands, $\Delta\nu = 220$ cm^{-1}, is very close of 223 cm^{-1} found for potassium terephthalate, a reference basis to apply Nakamoto's assignment principles of different coordination modes. The $-COO^-$ groups in the title compound should have a bridging character with the two oxygen atoms involved in different cobalt ions. From the three possible bridging terephthalate coordination modes depicted in Scheme 1, only type c was found to be present in $Co_2(OH)_2(C_8H_4O_4)$ (see later). In fact, for different carboxylates, the $\Delta\nu$ values for $-COO$ groups are different (for example, 164 cm^{-1} for sodium acetate, 201 cm^{-1} for sodium formate and 223 cm^{-1} for potassium terephthalate), depending on which molecular unit is attached to the carboxylate function. Ignoring this reference basis, erroneous attributions of $-COO$ coordination modes may be committed, leading to structural models open to criticism.[11e,f]

II.3.3. UV−Vis. Figure 3 shows the UV−vis absorption spectra of $Co_2(OH)_2(C_8H_4O_4)$, exhibiting light pink color. The recording for crystalline cobalt hydroxochloride $Co_2(OH)_3Cl$, used as a reference (upper curve), corresponds to octahedral cobalt ions with valence state +2. The title compound (bottom curve) shows a similar spectra, confirming the octahedral surrounding of Co(II) ions, with however a more complex profile in accordance with a distortion of coordination polyhedra, and/or spin forbidden transitions. The above bands are assigned to the d−d electronic transitions of octahedral cobalt(II) ion:[16] 500 and 550 nm for $^4T_{1g}(F) \rightarrow {}^4T_{1g}(P)$, 630 nm for $^4T_{1g}(F) \rightarrow {}^4A_{2g}(F)$, and 1200 nm for $^4T_{1g}(F) \rightarrow {}^4T_{2g}(F)$. For an octahedral surrounding, the values 754 and 910 cm^{-1} are deduced for D_q and B Racah's parameter, respectively.

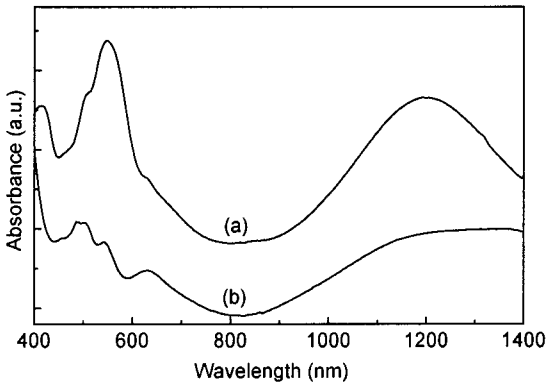

Figure 3. UV−vis absorption spectrum of $Co_2(OH)_3Cl$ (a) and $Co_2(OH)_2(tp)$ (b).

II.3.4. Ab-Initio Structure Determination from XRPD. Standard peak search methods were used to locate the diffraction maxima. TREOR[17] succeeded in finding a unit cell of approximate lattice parameters $a = 19.90$ Å, $b = 3.28$ Å, $c = 6.28$ Å, $\beta = 95.7°$, [$M(20) = 21$; $F(20) = 29$ (0.014, 48)] consistent with two formula units per unit cell. The analysis of the systematic absences indicated *C*2/*m* as probable space group, later confirmed by successful structure solution and refinement. However, since only a partial model could be initially obtained in *C*2/*m* by EXPO,[18] structure solution was attempted in the subgroup *P*2/*a*, with direct methods locating two independent Co atoms (of crystallographic site symmetry 2) and their full coordination spheres (three oxygen atoms). Difference Fourier maps revealed the location of the missing C atoms, showing that terephthalate moiety lies about an inversion center. With such a model, terephthalate ions, which are ∼24° off the (010) plane, bridge CoO_x layers which are ∼9.9 Å ($^1/_2$**a**) apart, connecting cobalt atoms which are shifted by $^1/_2$(**a** + **b** + **c**). The detailed analysis of the powder pattern, however, revealed that *no reflection* violating the C-centering conditions could be observed, while the *P*2/*a* model requires weak, but observable, extra peaks. Accordingly, we decided to work in the *C*2/*m* space group, later confirmed by full refinement and by the analysis of the possible pseudoequivalent 3D topologies, by introducing the disordering mirror plane which doubles the orientation of the tp fragments.

The final model was obtained by GSAS,[19] using the Rietveld technique and restraints on the variation of chemically known and stiff moieties, such as the organic part, for which a standard literature geometry was assumed. Figure 4 shows the final plot; crystal data, structure refinement parameters, and profile agreement factors can be found in Table 1, while fractional atomic coordinates are collected in Table 2.

III. Results and Discussion

III.1. Crystal Structure. The title compound is better described by a $Co_2(\mu_3\text{-}OH)_2(\mu_6\text{-}\eta^1,\eta^2,\eta^1,\eta^2\text{-tp})$ formulation, i.e. by octahedrally coordinated Co(II) ions (of *2*/*m* crystallographic symmetry), bearing either triply bridging hydroxyls and ($\mu_3\text{-}\eta^1,\eta^2$) carboxylato groups. Two crystallographically independent Co(II) ions are present: one bound by four hydroxyls and two carboxylic oxygen atoms, the other bearing two OH and four tp oxygen atoms. The tp anions are located about −1 symmetry element (4f position) and are bent ∼24° from the mirror plane in (010); therefore, they are disordered

(15) Nakamoto, K. *Infrared and Raman Spectra of Inorganic and Coordination Compounds*, 4th ed.; John Wiley & Sons: New York, 1986.

(16) Lever, A. P. B. *Inorganic Electronic Spectroscopy*; Elsevier: Amsterdam, 1986.

(17) Werner, P. E.; Eriksson. L.; Westdahl, M. *J. Appl. Crystallogr.* **1985**, *18*, 367−370.

(18) Altomare, A.; Burla, M. C.; Cascarano, G. L.; Giacovazzo, C.; Guagliardi, A.; Moliterni, A. G. G.; Polidori, G.; Rizzi, R.; Camalli, M. *J. Appl. Crystallogr.* **1999**, *32*, 339−340.

(19) Larson, A. C.; Von Dreele, R. B.; LANSCE, MS-H805, Los Alamos National Laboratory, Los Alamos, NM, 1990.

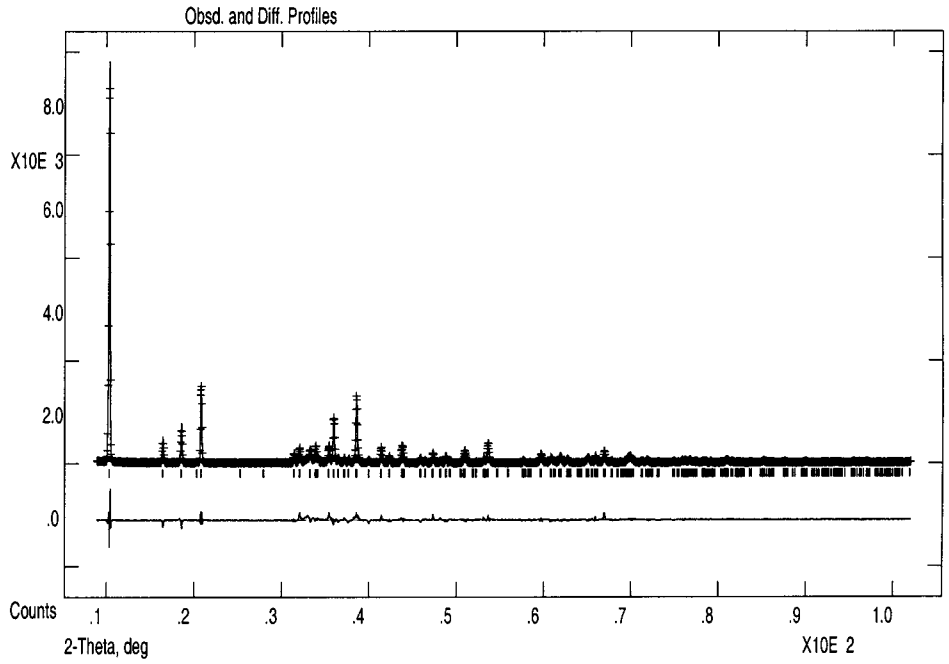

Figure 4. Rietveld refinement plot for $Co_2(OH)_2(tp)$, with peak markers and difference plot at the bottom.

Table 1. Crystal Data and Structure Refinement Parameters

compound	$Co_2(OH)_2(C_8H_4O_4)$
formula	$C_8H_6Co_2O_6$
fw, g mol^{-1}	316.00
system	monoclinic
space group	*C*2/*m*
a, Å	19.943(1)
b, Å	3.2895(1)
c, Å	6.2896(3)
β, deg	95.746(3)
V, Å^3	410.54(3)
Z	2
ρ_{calc}, g cm^{-3}	2.556
2θ range, deg	9.0−102.0
N_{obs}	9301
N_{ref}	178
$N_{restraints}$	11
R_p	0.158
R_{wp}	0.229
χ^2	3.27
R_F	0.118

Table 2. Fractional Atomic Coordinates for $Co_2(OH)_2(C_8H_4O_4)$ (esd's in Parentheses)

name	*x*	*y*	*z*	SOF
Co1	0.000000	0.000000	0.000000	1.0
Co2	0.000000	0.500000	0.500000	1.0
O1	0.0704(5)	0.000000	0.4506(14)	1.0
O2	0.1015(4)	0.000000	0.1301(13)	1.0
O3	0.0341(5)	0.500000	0.8098(16)	1.0
C1	0.11959(28)	0.000000	0.3344(16)	1.0
C2	0.19022(39)	0.083(5)	0.4188(12)	0.5
C3	0.26875(43)	0.236(4)	0.7199(9)	0.5
C4	0.20443(47)	0.102(6)	0.6387(11)	0.5

over two equiprobable sites. Such disorder is, however, conditioned since, down **b**, all tp fragments must be coherently tilted by the same amount, while neighboring stacks (in the **a** and **c** directions) may occasionally revert the sequence. For sake of simplicity, the drawing of Figure 5 is based upon an *ordered P*2/*a* space group, but, as confirmed by the diffraction pattern (see above), coherence is lost between the up and down tilts in the real sample, for which an *average C*2/*m* structure is found.

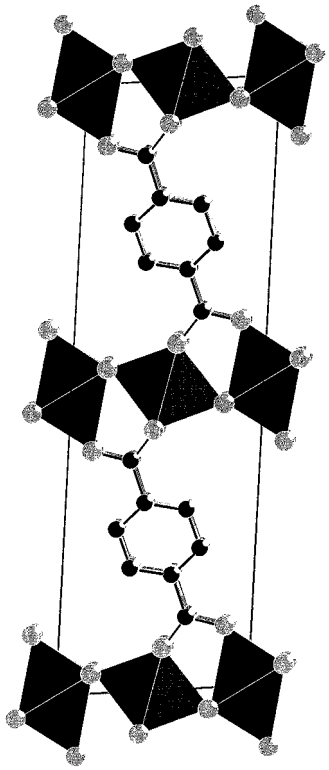

Figure 5. Crystal structure of $Co_2(OH)_2(tp)$, viewed down [010]. Relevant bond distances (Å) and angles (deg) are as follows: Co1−O2, 2.105(9), Co1−O3, 2.182(6), Co2−O1, 2.204(6), Co2−O3, 2.00(1); *cis*-O−Co1−O, 82.2(4)−97.8(4), *cis*-O−Co2−O, 83.5(3)−96.5(3), O1−C1−O2, 114.3(7). CoO_6 octahedra are shaded.

It is to be noted that zinc derivative of nominal composition $Zn_2(OH)_{1.76}(C_8H_4O_4)_{1.12}$[20] was found to possess a basal spacing of 13.3 Å and, therefore, cannot be considered to be isostructural to $Co_2(OH)_2(C_8H_4O_4)$.

The distances between cobalt(II) ions are shown to be in the range 3.20−3.55 Å, and so are much larger than 3.15 Å found in the Co(μ_3-OH)$_2$ layers of the parent hydroxide $Co(OH)_2$[21] (see Figure 6). These differences

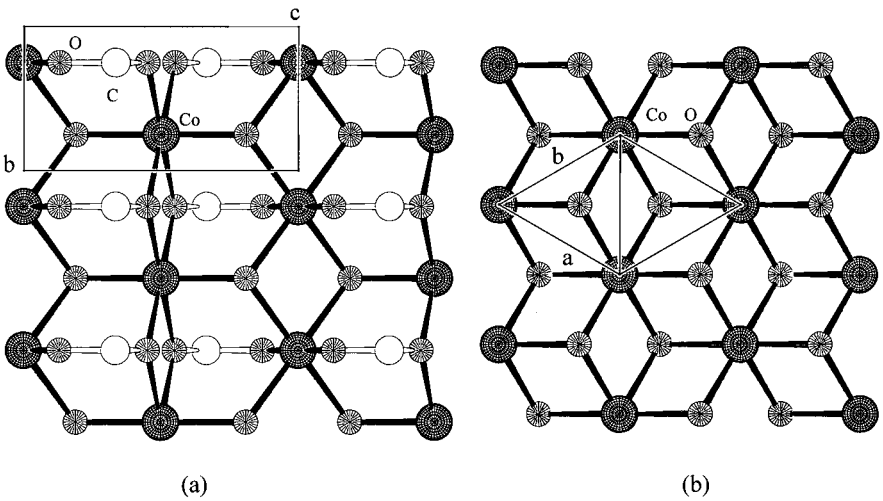

Figure 6. Sketch of the CoO_x layers found (a) in the title compound (down [100], ring C atoms omitted) and (b) in trigonal $Co(OH)_2$ (down [001]).

can be attributed to the different hapticity of the tp anion, which, substituting one μ_3-OH group with a μ_3,η^2,η^1-O_2CAr fragment, inflates the metal ion packing. The major consequences of such novel RCO_2 μ_3,η^2,η^1-coordination mode, which should not be typical for the tp ion alone, are (i) the above-mentioned unequivalence of Co(II) ions; (ii) the significant tilting of the originally equioriented CoO_6 octahedra (the layer reported in Figure 6a clearly contains juxtaposition of columns of different kind), and possibly, (iii) the significant changes in the magnetic properties from large magnetocrystalline anisotropy and noncollinear spin arrangement. The fact that carboxylates such as to bind CoO_x sheets in this manner is not obvious, until a full structural analysis is performed, nor can this structural study be taken as "general", since we have already shown that acetate in $Cu_2(OH)_3(O_2CCH_3)\cdot H_2O$[22] coordinates through a single oxygen atom. Possibly, the difference relies on the different $[M_2(OH)_2(carboxylate)_2$ vs $M_2(OH)_3(carboxylate)]$ stoichiometry. Worthy of note, such an unusual carboxylate coordination has also been evidenced for the succinate-based compound $Co_5(OH)_2(C_4H_4O_4)_4$.[23]

After idealizing the location of the unobservable H atom of the unique μ_3-OH group, the analysis of the shortest contacts reveals only oxygen atoms at distances higher than 2.5 Å, thus indicating that H atoms are not involved in any hydrogen-bond interaction with neighboring carboxylates. Also, among the peculiar structural features of the title compound, a rather short $\pi-\pi$ stacking between parallel, *but offset* (hence possibly attractive[24]), adjacent aromatic rings is found (~3.06 Å), which may justify the apparent stiffness of the crystal phase, witnessed by its sharp XRPD peaks, and its high thermal stability.

As previously demonstrated for similar zinc[20] and copper[25] hydroxy derivatives with monocarboxylate anions, layered organic/inorganic hybrids may be isolated whose structural features can partially be foreseen on the basis of simple rules.[1,20,25] Upon extending such rules to α,ω dicarboxylates, grafting of both ends generally increases the dimensionality and stability of the network.[23,26] When stiff, but polarizable aromatic units are introduced, then specific structural (short $\pi-\pi$ stacks) and/or magnetic properties may result, not accessible in their aliphatic or simpler congeners (see below). In particular, it has been demonstrated in binuclear complexes that tp anion linking only two metals in the (μ_2-η^2-η^2) mode affords very weak exchange interaction.[27,28] Similarly, only limited coupling is observed for 1D systems involving (μ_2-η^1,η^1) tp ions, like $Cu(H_2O)_2(tp)$.[29] For (μ_4-$\eta^1,\eta^1,\eta^1,\eta^1$) tp moieties bridging Mn(II) complexes in a polymeric fashion, much more efficient exchange coupling can be found.[27,30] Thus, the magnetic interactions between "single layer magnets", mediated by tp ion in $Co_2(OH)_2(C_8H_4O_4)$, may be favored by their polybridging (μ_6-$\eta^1,\eta^2,\eta^1,\eta^2$) character.

Once again, when single crystals cannot be grown, ab initio XRPD structure determination, recently reviewed by us[31] and others[32] in the field of coordination chemistry, has proven to successfully substitute more standard diffraction methods. Basically, the molecular complexity must be not too high, and well conditioned and conventional laboratory equipments are needed. As often observed for structures refined from X-ray powder data only, absolute geometric parameters (bond distances and angles) are somewhat in error, due to the

(20) Ogata, S.; Tagaya, H.; Karasu, M.; Kadokawa, J. *J. Mater. Chem.* **2000**, *10*, 321−327.
(21) (a) Lotmar, W.; Feitknecht, W. *Zeit. Kristall. Kristallgeom. Kristallphys. Kristallchem.* **1936**, *93*, 368−378. (b) Wells, A. F. *Structural Inorganic Chemistry*, 5th ed.; Clarendon Press: Oxford, 1995; p 631.
(22) Masciocchi, N.; Corradi, E.; Sironi, A.; Moretti, G.; Minelli, G.; Porta P. *J. Solid State Chem.* **1997**, *131*, 252−262.
(23) Livage, G.; Egger, C.; Ferey, G. *Chem. Mater.* **1999**, *11*, 1546−1550.
(24) Hunter, C. A.; Sanders, J. K. M. *J. Am. Chem. Soc.* **1990**, *112*, 5525−5534.
(25) Fujita, W.; Awaga, K. *Inorg. Chem.* **1996**, *35*, 1915−1917.
(26) Morioka, H.; Tagaya, H.; Karasu, M.; Kadokawa, J.; Chiba, K. *J. Mater. Res.* **1998**, *13*, 848−851.
(27) Cano, J.; De Munno, G.; Sanz, J. L.; Ruiz, R.; Faus, J.; Lloret, F.; Julve, M.; Caneschi, A.; *J. Chem. Soc., Dalton Trans.* **1997**, 1915−1923.
(28) Erasmus, C.; Haase, W. *Spectrochim. Acta, Part A* **1994**, *50*, 2189−2195.
(29) Deakin, L.; Arif, A. A.; Miller, J. S. *Inorg. Chem.* **1999**, *38*, 5072−5077.
(30) Cano, J.; De Munno, G.; Sanz, J.; Ruiz, R.; Lloret, F.; Faus, J.; Julve, M. *J. Chem. Soc., Dalton Trans.* **1994**, 3465−3469.
(31) Masciocchi, N.; Sironi, A. *J. Chem. Soc., Dalton Trans.* **1997**, 4643−4650.
(32) Poojary, D. M.; Clearfield, A. *Acc. Chem. Res.* **1997**, *30*, 414−422.

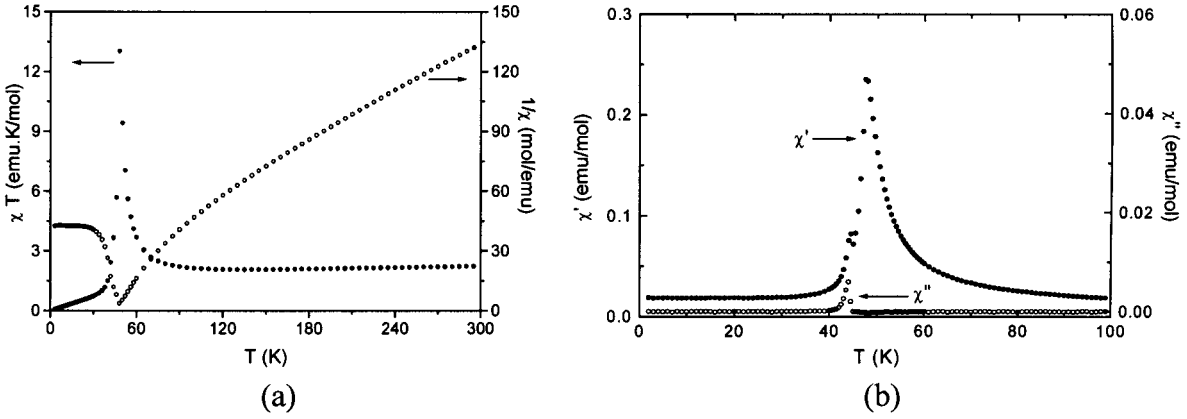

Figure 7. Temperature dependence of the static χ^{-1} and χT at 50 Oe (a) and of the ac susceptibility under a 3.5 Oe alternating field at 20 Hz (b) for $Co_2(OH)_2(tp)$.

intrinsic limitations of the method. However, when average values of chemically equivalent descriptors are computed or, even better, when the structural features concern atoms on special positions and/or polymeric links (necessarily imposing stiff boundary constraints),[33] such underdetermination is reduced.

In addition, the use of reference values (such as those derived from a CCDC search for the tp group—362 hits) cannot worsen the model definition, since their validity ranges are well contained within the possible spread of IAM refinements, granting superior results for "*free*" parameters derived therefrom. Accordingly, we confidently trust, even in the presence of mentioned disorder, the Co—O environments discussed above, which most of the magnetic properties of our sample are likely to depend on. Moreover, the 3D structure depicted in Figure 5 adds new important knowledge (stoichiometry, topology, intermolecular contacts) to this class of organic—inorganic hybrids, well beyond the widespread 2D sketches,[1,11d,25,34] mainly based on the observation of "00*l*" spacing(s) alone, which, however convey important structural information.

III.2. Magnetic Properties. The temperature dependence of the magnetic susceptibility of a powder sample, measured at $H = 50$ Oe, is plotted in Figure 7a as $\chi T = f(T)$ and $1/\chi = f(T)$. χT slightly decreases from 2.23 emu K mol^{-1} at room temperature down to 2.06 emu K mol^{-1} at 135 K, and then it exhibits a significant increase on further cooling up to a sharp maximum at 48.0 K, characteristic of a magnetic long-range ordering. At lower temperatures, χT decreases rapidly to zero. The fit of $\chi^{-1}(T)$ in the range 200—300 K, using the Curie—Weiss expression, gives $\theta = -40.6$ K and the effective moment $\mu_{eff} = 4.51\ \mu_B$. This value falls in the range of the expected values of 4.30—5.20 μ_B for the high-spin Co^{2+} ion.[35]

The temperature dependence of the ac susceptibility (Figure 7b) measured in a field of ±3.5 Oe shows the same features. The maximum of χ' observed at $T_c = 47.8$ K, in agreement with the above results, confirms the occurrence of a phase transition. The absence of out-of-phase signal (χ'') at this temperature points to a long-range antiferromagnetic order. However, the imaginary component χ'' presents a peak at 44.0 K, which is a signature of a magnetized state, indicating that a partly canted antiferromagnetic structure takes place below this temperature. No frequency dependence of these transitions is observed.

The influence of the applied field on the magnetic order has been studied from the field dependence of magnetization $M(H)$.The $M(H)$ plots are shown to depend closely on the temperature range, as illustrated in Figure 8 for some selected temperatures. Three regions may be distinguished upon cooling from the ordering temperature.

1. In the range 48—45 K, the magnetization exhibits a linear variation in low field, and then a characteristic metamagnetic transition, i.e., a rapid rise of the moment at a critical field (ranging from 0.17 to 0.28 T), corresponding to the stabilization of a magnetized state. No magnetic hysteresis is detected, as shown in Figure 8a for the plot at $T = 45$ K. The magnetization value reached after the transition is still well below that expected for a Co(II) ion, even in its spin $^1/_2$ ground-state (~1.8 μ_B). Hence the spin configuration of the excited state is most likely noncollinear.

2. Between 45 and 30 K, the steplike transition is always noticeable with a turn upfield increasing from 0.28 T (45 K) to 0.45 T (30 K). However the metamagnetic transition is now hysteretic, as shown in Figure 8b for 40 K, and the hysteresis increases continuously with decreasing temperature. The true threshold field, which would be about halfway between the turn up and turn down thresholds, varies very little. In this temperature range a very small remnant moment is also observed, which reaches at most 0.05 μ_B/Co(II)mol at 30.0 K. The compound is thus a weakly canted antiferromagnet, which will be referred to as CAF1 hereafter.

3. Below 30.0 K, the first magnetization curves are still S-shaped. Upon lowering the temperature, the hysteresis cycle opens very quickly, the turn down threshold field becomes negative, the remnant moment and the coercive field increase rapidly. Figure 8b shows an example at 24.0 K for which $M_{rem} = 0.27\ \mu_B$/Co(II)-mol and $H_c = 0.47$ T. Below 24 K, the metamagnetic thresholds become ill-defined as they are closer and closer to the coercive field. Because of the increasingly

(33) Masciocchi, N.; Ardizzoia, G. A.; Maspero, A.; La Monica, G.; Sironi, A. *Inorg. Chem.* **1999**, *38*, 3657—3664. Masciocchi, N.; Ardizzoia, G. A.; La Monica, G.; Maspero, A.; Sironi, A. Submitted for publication, 2000.

(34) Kurmoo, M.; Day, P.; Derory, A.; Estournès, C.; Poinsot, R.; Stead, M. J.; Kepert, C. J. *J. Solid State Chem.* **1999**, *145*, 452—459.

(35) Carlin R. L. *Magnetochemistry*; Springer-Verlag: Berlin/Heidelberg, 1986.

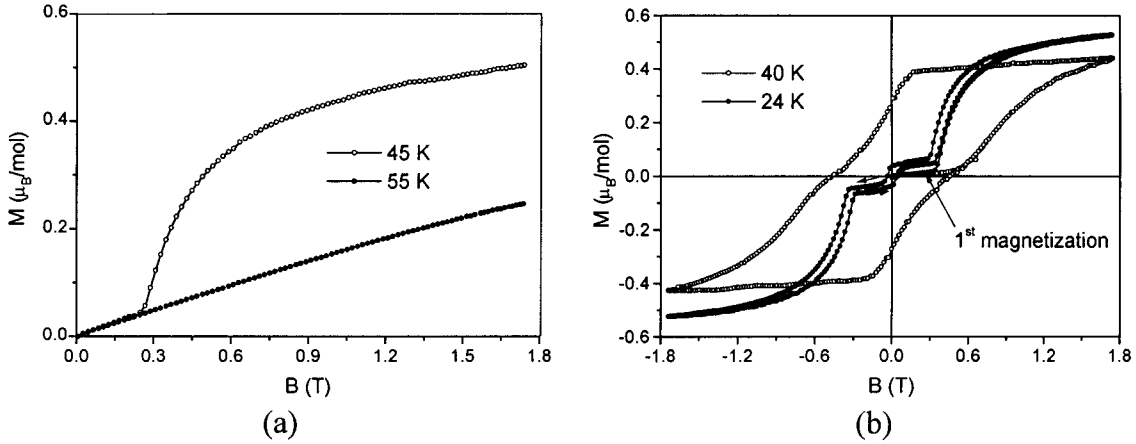

Figure 8. Field-dependent magnetization of $Co_2(OH)_2(tp)$, at 55, 45 K (a) and 40, 24 K (b). Note: the high field reversible part of the curve is not reached at 24 K.

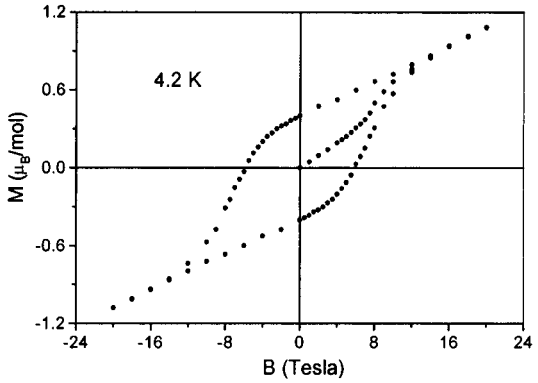

Figure 9. High field magnetization up to 20 T for $Co_2(OH)_2$-(tp) at 4.2 K.

large anisotropy, $M(H)$ curves do not reach their reversible part below 1.8 T, and, accordingly, the coercive field and the remnant moment are not reliable. High field magnetization measurements performed up to 20 T give more insight on the actual magnetic features (Figure 9). A giant hysteretic effect is observed at 4.2 K, with a value of the coercive field $H_c = 5.9$ T, pointing to a very large magnetic anisotropy, in relation with the spin−orbit coupling effect and the influence of dicarboxylate anions on the site symmetry. Note that the magnetostatic anisotropy also contribute to the hysteretic effect, but, in the present case, it does not exceed 500 G for randomly orientated acicular particles. It may be emphasized that full saturation is not yet reached at 20 T because of both the large spin−orbit splitting of the cobalt(II) levels and the antiferromagnetic exchange coupling between layers. The net moment in low field $M_{rem} = 0.40\ \mu_B$/Co(II)mol indicates that the spin configuration at that temperature is still noncollinear, but with a larger canting angle compared to the previous state. It is hereafter referred to as CAF2.

The temperature dependence of the remnant magnetization shown in Figure 10a illustrates very clearly the existence of a magnetized structure order with a net moment below 45 K. The remnant moment stays small in the CAF1 phase down to about 30 K where it exhibits a change of regime, and rises quickly up to a plateau in the CAF2 phase below 15 K.

From the above findings, it can be deduced that $Co_2(OH)_2(C_8H_4O_4)$ is well described at high temperature by quasi-isolated cobalt(II) ferromagnetic layers. The in-plane interaction may be approximated from the model developed by Suzuki et al. from the Green's function technique.[36] Using the expression $\chi T \sim \exp(2\pi JS^2/kT)$ proposed for isotropic spins, we deduce the coupling constant $J = 18.9$ K.

The phase transition observed at 48 K indicates clearly that antiferromagnetic interlayer interactions take place, likely due to the influence of the conjugated π electrons of the terephthalate anion. Such a behavior has already been reported for the related copper(II) compound with the dicarboxylate anion $CO_2C_4H_4CO_2^{2-}$, characterized by a similar basal spacing ($d = 10.4$ Å).[13] Indeed the interlayer exchange interaction due to the spin polarization through the bridging anion is expected to favor an antiferromagnetic order. The fact that upon cooling below 45 K a net and small moment is stabilized in the ground-state points to a competition between the antiferromagnetic exchange coupling and the single-ion anisotropy, which would be responsible for an uncompensated noncollinear magnetic structure. Although there are two kinds of octahedrally coordinated cobalt sites with different degrees of anisotropy and different orientation within the layers, a possible noncollinearity of the moments within the same layer cannot explain the observed net moment. Indeed there would still be a one to one compensation between moments of the same kind in adjacent layers. Therefore, one must assume that the easy axis of the equivalent Co sites is tilted every other layer.

The abrupt change of regime observed below 30 K could be associated, as a first guess, with either a crystallographic or a magnetic transition. Very low temperature XRD is required to support the first explanation. However there is no need for such structural transition to explain the experimental observations. Indeed, as quoted above, the hysteresis of the metamagnetic transition increases continuously as the temperature decreases. This is related to the progressive emptying of the excited states in the spin−orbit split multiplet of Co(II), which leads to a regular increase of the single ion anisotropy. As a consequence the turn down threshold field of the metamagnetic transition crosses the $B = 0$ axis in the vicinity of 30 K. Therefore, our favored explanation would be merely that the spin

(36) Suzuki, F.; Shibata, N.; Ishii, C. *J. Phys. Soc. Jpn.* **1994**, *63*, 1539−1547.

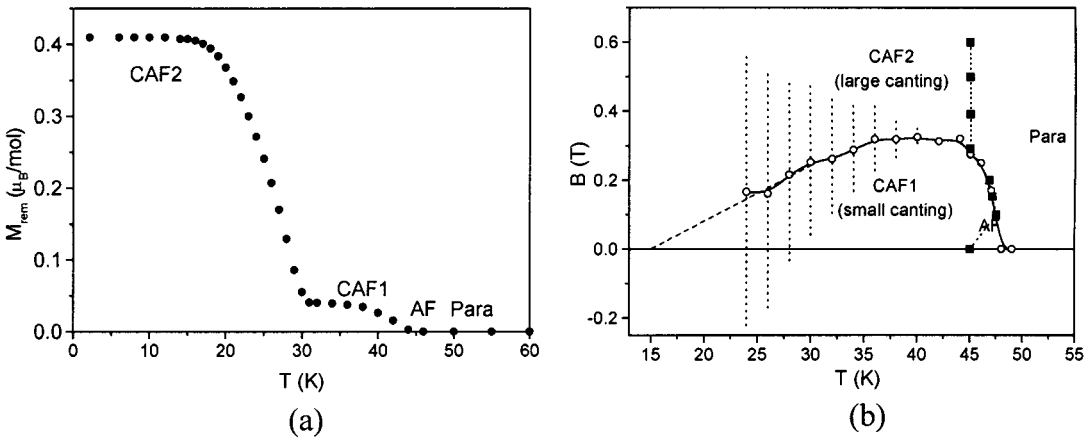

Figure 10. Temperature dependence of the remnant moment (a) and magnetic phase diagram (b). Open circles: threshold field of the metamagnetic transition, the vertical dotted bars indicate the hysteresis of the transition, the dashed line is a speculated extrapolation. Full squares: peak of the imaginary part of the ac susceptibility.

structure stabilized in high fields remains metastable down to more and more negative fields below 30 K. But the ground-state phase would still be the CAF1 one down to 15 K, as suggested by the two stages of the magnetization reversal (see Figure 8b).

Below 15 K the magnetization reversal takes place in one step from the positive canted state to the negative one. Then the CAF2 structure is probably stable in any field.

Summarizing, the magnetic structure of the title compound can be understood as arising from a ferromagnetic exchange interaction within the layer and an antiferromagnetic coupling between the layers, leading to an antiferromagnetic 3D order below 48 K. On top of this overall antiferromagnetic structure the thermal variation of the magnetic anisotropy gives rise to three possible spin arrangements that are nearly degenerated: (a) plain antiferromagnetic between 48 and 45 K where the ferromagnetic layers are fully compensated; (b) weakly canted antiferromagnetic with nearly compensated ferromagnetic layers between 45.0 and 30.0 K, and (c) strongly canted antiferromagnetic below 15 K. Between 30 and 15 K the last structure is responsible for a large remnant magnetization but it is probably only metastable in zero field; this is still a matter of further investigations. Figure 10b gives the relevant magnetic phase diagram built from the critical fields for the metamagnetic transition and the ac susceptibility measurements made under an applied static field at different temperatures.

IV. Conclusions

The concept of self-assembling in crystal engineering via hydrothermal synthesis has been successfully used to synthesize a new terephthalate-based hybrid magnet $Co_2(OH)_2(C_8H_4O_4)$, in which the terephthalates are coordinated and pillared to the hydroxide layers. Structural studies show that the strong iono−covalent bond interactions between organic components and inorganic layers are established. Large distortions and different orientations of Co(II) octahedra and different exchange pathways among cobalt ions are found within the inorganic layers. On the basis of such a structural type, very unusual magnetic properties, like different magnetization curves below $T_N = 48.0$ K and giant hysteretic effects up to 5.9 T at 4.2 K, are observed. Referring to the precedent works on cobalt hydroxide-based hybrid materials, $Co_2(OH)_2(C_8H_4O_4)$ is the first example of spin layers interconnected through π electron ligands, with an overall description of both structure and magnetic properties. Studies on other transition metal ions and other organic components such as biphenyl-4,4′-dicarboxylic and benzoic anions are in progress; preliminary results showed that the cobalt hydroxy derivatives of these anions are ferromagnets with $T_c = 34.0$ and 38.0 K, and coercive fields of 4.4 T (at 4.0 K) and 900 Oe (at 2.0 K), respectively, but will be reported in a forthcoming paper, together with details on the design of new high T_c 2D hybrid compounds and with their complete magnetic characterization.

Acknowledgment. The authors thank Dr. R. Poinsot and A. Derory for their help in magnetic measurements, and E. Chappel and G. Chouteau for the high field experiment in Grenoble HMF laboratory. CNRS is acknowledged for the grant for Z.L.H. This work was supported within the frame of the “Programme Matériaux” from CNRS.

CM000386C